Equilibrium Partitioning of Flexible Macromolecules in Fibrous Membranes and Gels

Jeffrey A. White[†] and William M. Deen*[,†,‡]

Department of Chemical Engineering and Division of Bioengineering and Environmental Health, Massachusetts Institute of Technology, Cambridge, Massachusetts 02139

Received May 22, 2000; Revised Manuscript Received August 28, 2000

ABSTRACT: A theory was developed to describe the equilibrium partitioning of a flexible polymeric solute between a dilute solution and a medium consisting of a randomly oriented array of fibers (e.g., a fibrous membrane or gel). The fibers were regarded as long, rigid cylinders, and the solute was modeled as a chain consisting of n mass points joined by $n - 1$ rectilinear segments. Results were obtained for freely jointed chains and for chains with fixed bond angles, using a combination of analytical and computational (e.g., Monte Carlo) techniques. The predicted partition coefficient (Φ, the solute concentration in the fibrous material divided by that in the bulk solution) proved to be sensitive to the number of fibers included; typically, 50 or more nearest-neighboring fibers were needed to obtain a convergent result. The values of Φ decreased as fiber volume fraction, molecular size, or number of mass points was increased selectively. As the bond angle was increased from 0° (a chain folding back on itself) to 180° (a rodlike chain), Φ first decreased and then increased. The model predictions agreed reasonably well with literature partitioning data for various polymeric solutes in hydrogels, especially when the radius of gyration was no more than a few times the fiber radius. With the radius of gyration specified, the model predictions were fairly insensitive to whether the bond angle was fixed or random.

Introduction

The equilibrium distribution of a macromolecule between a solution and a porous or fibrous material is a critical factor in size-exclusion chromatography and in certain membrane-based separation processes. Accordingly, there is considerable interest in predicting how the partition coefficient will depend on molecular size and other parameters. The partition coefficient (Φ) is the concentration of the macromolecular solute in the confined phase (chromatography bead or membrane) divided by that in the bulk solution, at equilibrium. For fibrous membranes and gels, which are the focus of the present work, the concentration in the confined phase is based on the total volume (including solids).

Fibrous materials and polymeric gels often have disordered structures, which suggests that they be modeled as arrays of randomly oriented fibers with fluid-filled interstices. The simplest approach is to assume that the fibers are rigid and of uniform size. The partitioning of macromolecules in such a system was investigated first by Ogston,[1] who used geometric arguments to derive the probability density for encountering the closest fiber at a given distance from an arbitrary point. Integrating that probability density over all possible separation distances yielded the partition coefficient for a spherical molecule. The result was

$$\Phi = \exp\left[-\phi\left(1 + \frac{r_s}{r_f}\right)^2\right] \qquad (1)$$

where r_s and r_f are the solute and fiber radii, respectively, and ϕ is the volume fraction of fibers. Equation 1 illustrates the key feature of partitioning governed by steric interactions, namely, that Φ decreases with increasing molecular size. The validity of eq 1 for dilute solutions of spheres has been confirmed by Fanti and Glandt[2] and Lazzara et al.,[3] using other theoretical approaches. For concentrated solutions of macromolecules in equilibrium with fibrous media, results have been obtained for uniform spheres[2] and for mixtures of rigid particles of arbitrary shape.[3] There is an analysis also for arrays of charged fibers in contact with dilute solutions of charged spheres.[4]

In contrast to the situation for rigid macromolecules, there appear to be no theoretical results for the partitioning of flexible polymers in random fiber arrays. For linear polymers with many possible conformations, analyses have been limited to pores of uniform cross section. In one of the earliest studies, Casassa[5] showed that the partition coefficient for a random-flight chain in a cylindrical pore could be calculated by solving a partial differential equation analogous to that which governs transient heat conduction or diffusion in a rod. That approach was extended later to describe the partitioning of linear polyelectrolytes in charged pores.[6] As discussed in Chandrasekhar,[7] such continuum formulations are valid for chains having infinitely many segments of vanishingly small length. The effects of finite numbers of chain segments and finite segment lengths were explored for random-flight polymers in cylindrical pores by Davidson et al.,[8] using a Monte Carlo technique. For a chain with a specified number and length of segments, a representative population of chain conformations was generated, and each conformation tested to estimate the probability of successfully fitting such a chain in a given pore. For the same radius of gyration, it was found that values of Φ for chains with finite numbers of segments tended to exceed those predicted by the continuum formulation. The differences between the continuum and Monte Carlo results were often quite large.

A theory for the partitioning of linear polymers in fiber matrices would be useful, for example, in the

[†] Department of Chemical Engineering.
[‡] Division of Bioengineering and Environmental Health.
* Address for correspondence: Telephone (617) 253-4535; Fax (617) 258-8224; E-mail wmdeen@mit.edu.

10.1021/ma0008793 CCC: $19.00
Published on Web 10/07/2000

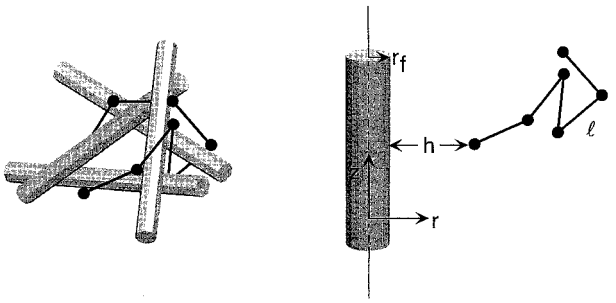

Figure 1. Left: schematic of a polymer chain interacting with multiple fibers. Right: computational domain used to evaluate the probability that a chain will avoid overlap with a given fiber. A chain with five segments ($n = 6$), each of length l, is shown with one end at a distance h from a fiber of radius r_f. Cylindrical coordinates (r, z) are centered on the fiber.

analysis of size-exclusion chromatography results, in the characterization of synthetic membranes, and in the interpretation of microvascular permeability data obtained using exogenous polymeric tracers (e.g., dextran). The objective of the present study was to predict values of Φ for dilute solutions of polymers in media consisting of randomly oriented fibers. Results were obtained both in the limit of infinitely many segments (using a continuum formulation) and for finite numbers of segments (using a Monte Carlo method). After the methodology is described, some general results are presented to illustrate the effects of radius of gyration, number of segments, r_f, and ϕ on partitioning. The predictions are then compared with several sets of published data on the partitioning of linear polymers in gels, and the strengths and limitations of the theory are discussed.

Model Formulation and Computational Methods

Overall Formulation. The fibers in the membrane or gel were modeled as straight, infinitely long cylinders of radius r_f, with random orientations. The macromolecular solutes were represented as chains consisting of n mass points joined by $n - 1$ rectilinear segments, each of length l. For freely jointed chains, the radius of gyration (r_g) is given by[9]

$$r_g = \left[\frac{(n-1)(n+1)}{6n}\right]^{1/2} l \tag{2}$$

For chains with free rotation of any given segment at a fixed bond angle, β, the corresponding result is[10]

$$r_g = \frac{l}{n}\{\sum_{j=1}^{n}\sum_{i=1}^{j-1}[j - i + 2\sum_{k=1}^{j-i-1}(j - i - k)(-\cos\beta)^k]\}^{1/2} \tag{3}$$

The bond angle is defined such that $\beta = 0$ for a segment that doubles back on the previous one, and $\beta = \pi$ for a straight, rodlike arrangement. The bulk solution was assumed to be dilute enough that interactions among polymer chains could be neglected, leaving only polymer−fiber interactions to be considered.

A key aspect of such systems is that the dimensions of the polymer chain may exceed typical interfiber spacings, causing the chain to interact simultaneously with several fibers, as illustrated in Figure 1 (left). The position of a flexible polymer is described most conveniently by choosing one end of the chain as the locator point. The fibers in the vicinity of that end of the chain are then identified as the nearest, second-nearest, third-nearest, etc., to the locator point. In testing whether a chain with a particular conformation will fit at a given location, the steric interactions with each fiber can be viewed as independent events. Accordingly, the partition coefficient is given by

$$\Phi = \Phi_1\Phi_2\Phi_3\ldots = \prod_{i=1}^{\infty}\Phi_i \tag{4}$$

where Φ_i is the probability that an arbitrarily placed chain will successfully avoid overlap with the ith nearest-neighboring fiber. If $p(s)$ is the probability that a random-flight chain with one end at a distance s from the surface of a fiber will not overlap anywhere with that fiber, and if $g_i(s)$ is the probability density function describing the distance of the ith nearest-neighboring fiber from an arbitrary point in the fiber matrix, then

$$\Phi_i = \int_0^{\infty} p(s)\, g_i(s)\, \mathrm{d}s \tag{5}$$

In other words, the probability of avoiding a given fiber is the expected value of $p(s)$, considering all possible separation distances. Distances here are scaled by the fiber radius, such that $s \equiv h/r_f$, where h is the dimensional distance to the fiber surface. Because the fibers are assumed to be of uniform size, the same function $p(s)$ applies to each. The evaluation of $g_i(s)$ is described next, and then the calculation of $p(s)$ is outlined.

The probability density function for the distance of the ith nearest-neighboring fiber was derived as follows. Let D be the nearest distance of a fiber axis from a reference point. For a population of randomly oriented fibers in three dimensions, Ogston[1] showed that the probability of encountering a fiber in a small interval $\Delta(D^2)$ is $2\pi CL\Delta(D^2)$, where C is the fiber concentration (number per unit volume) and $2L$ is the length of one fiber. Thus, when distance intervals are expressed in terms of D^2 (rather than D), the encounter probability happens to be independent of the absolute distance, D. We now imagine a process in which an interval $[0, D^2]$ is covered in m steps, each of "length" $\Delta(D^2) = D^2/m$. Because the probability of encountering a fiber in any one step is constant, the probability of encountering k fibers in m steps, denoted as $P_k(m)$, is given by a binomial distribution. The probability of encountering the kth fiber on the mth step, denoted as $F_k(m)$, is the probability that $k - 1$ encounters occurred through $m - 1$ steps, times the probability of an encounter on the mth step. It follows from the binomial distribution that

$$F_k(m) = \frac{k}{m}P_k(m) \tag{6}$$

In the limit $m \to \infty$, $P_k(m)$ becomes a Poisson distribution, the parameter in that distribution being m times the probability of an encounter in one step, or $2\pi CLD^2$.[11] The probability density function obtained from eq 6 is then

$$f_k(D^2) = \frac{(2\pi CL)^k}{(k-1)!}(D^2)^{k-1}\exp(-2\pi CLD^2) \tag{7}$$

$$\int_0^{\infty} f_k(D^2)\, \mathrm{d}(D^2) = 1 \tag{8}$$

As shown by eq 8, the distribution in eq 7 is properly normalized. The probability density function needed in

eq 5 is obtained by setting $D = h + r_f$ in eq 7 and noting that $\phi = 2\pi CLr_f^2$. The result is

$$g_k(s) = \frac{2\phi^k}{(k-1)!}(1+s)^{2k-1}\exp[-\phi(1+s)^2] \quad (9)$$

$$\int_0^\infty g_k(s)\,ds = 1 \quad (10)$$

It is worth noting that the probability density function derived by Ogston[1] for the fiber closest to a point is recovered by setting $k = 1$ in eq 7. The partition coefficient for a sphere (eq 1) is obtained by considering only the nearest fiber (i.e., $\Phi = \Phi_1$), and recognizing that p becomes a step function, with a value of zero for $D < r_f + r_s$ and a value of unity otherwise. Only one fiber is needed because a sphere is excluded whenever $D < r_f + r_s$ for *any* fiber, and (by definition) D is smallest for the nearest fiber.

The computational domain used to evaluate $p(s)$ was the unbounded region external to a solid cylinder of radius r_f, with the cylinder (fiber) centered at the origin and aligned with the z axis, as shown in Figure 1 (right). The cylindrical symmetry ensures that the probability of finding a macromolecular solute at a given position depends only on the radial coordinate, r. As described below, the continuum and Monte Carlo calculations differed only in the manner in which $p(s)$ was calculated. In either case, the values of Φ_i were computed by evaluating the integral in eq 5 numerically using Bode's law.[12] The relative error in Φ due to the numerical integration was estimated to be <1% for all cases, which is negligible compared to the errors associated with the evaluation of $p(s)$ and with the truncation of eq 4 at a finite number of terms. The number of terms needed in eq 4 depended both on λ and n, as will be discussed; as many as 90 terms were computed.

Continuum Method. For $n \to \infty$, $p(s)$ was calculated by solving a partial differential equation analogous to that describing transient heat conduction or diffusion in a region surrounding a cylinder. In this formulation, locations along a chain are described in terms of a continuously varying contour length, rather than discretely numbered mass points. The fractional contour length is given by τ, such that $\tau = 0$ at the locator end and $\tau = 1$ at the opposite end. A location on the chain corresponding to a particular value of τ is referred to simply as "point τ". The radial coordinate is scaled with the fiber radius, such that $\eta \equiv r/r_f$. The probability of finding point τ at position η, given that no preceding part of the chain overlaps with the fiber, is denoted as $P(\eta,\tau)$. As discussed in Casassa[5] and Lin and Deen,[6] the differential equation governing $P(\eta,\tau)$ is

$$\frac{\partial P}{\partial \tau} = \frac{\lambda^2}{\eta}\frac{\partial}{\partial \eta}\left(\eta\frac{\partial P}{\partial \eta}\right) \quad (11)$$

where $\lambda = r_g/r_f$. The required "initial condition" and boundary conditions are

$$P(\eta,0) = 1 \quad (12)$$

$$P(1,\tau) = 0 \quad (13)$$

$$P(\infty,\tau) = 1 \quad (14)$$

Equation 12 allows the locator end to sample all radial positions with equal probability;[6] the "absorbing wall" boundary condition, eq 13, has the effect of excluding all chain conformations that overlap with the fiber;[13] and eq 14 expresses the fact that a chain of any size will not be sterically excluded if it is sufficiently distant from the fiber.

An analytical solution to the analogous heat conduction problem has been reported,[14] but its form is not computationally convenient. We found it easier to evaluate $P(\eta,\tau)$ numerically using a finite difference technique; the Crank−Nicolson method was used.[12] Step sizes were chosen so that the errors associated with the numerical solution of eq 11 were negligible compared to the truncation errors in calculating Φ (see below). Once $P(\eta,\tau)$ was determined, the probability of successfully fitting the entire chain at position η was evaluated as $P(\eta,1)$. Given that $r = r_f + h$ (Figure 1) and $s = h/r_f$, it follows that

$$p(s) = P[(1+s),1] \quad (15)$$

Monte Carlo Method. For freely jointed chains with finite n, a Monte Carlo method was used to compute $p(s)$. Chain configurations were generated by choosing vectors of length l and random orientation and adding them end-to-end until the chain had the desired number of segments. The method used to generate the vectors, due to von Neumann, is described in Allen and Tildesley.[15] For chains with restricted bond angles, the previous segment was assumed to be aligned with the z axis of a local coordinate system, the segment extending from $z = l$ to the origin. Changing to a local set of spherical coordinates (r, θ, ϕ), the end of the current segment was found by setting $r = l$, $\theta = \beta$ and choosing a random value for ϕ in the interval $[0, 2\pi]$. The random number generator used ("ran2" in Press et al.[12]) provides about 2×10^{18} uncorrelated numbers between 0 and 1; this was adequate for our purposes, since the maximum number of calls to ran2 in any one simulation was $\sim 10^9$. Each chain configuration was tested by placing one end at a given dimensionless distance s from the fiber surface and determining whether any part of any segment fell within the fiber. The fraction of successful fits obtained with a large population of configurations was equated with $p(s)$. The method described in Davidson et al.[8] was used to estimate the error in each of the Φ_i. The error propagation scheme presented in Harris[16] was used to estimate the error in Φ. Simulations with 5000 chains were sufficient to limit the absolute and relative errors in Φ to ≤ 0.01 and $\leq 8\%$, respectively (95% confidence limit).

The possibility of directional bias in the orientation of chain segments was examined by computing $p(h/l)$ for a dumbbell ($n = 2$) adjacent to a plane wall. (The separation distance h is scaled here by l, because r_f is infinite.) Because the free end of the dumbbell should occupy, with equal probability, all points on the surface of a sphere of radius l, the fraction of allowed configurations is just the fraction of the sphere surface not cut off by the plane. For a plane located at a distance h ($\leq l$) from the sphere center, the ratio of the truncated to the complete area gives

$$p\left(\frac{h}{l}\right) = \frac{1}{2}\left(1 + \frac{h}{l}\right) \quad (16)$$

To test the algorithm used to identify a chain segment that overlaps with a fiber, $p(h/l)$ was computed also for a rod adjacent to a long cylinder of radius r_f. The truncated area for this case was computed numerically.

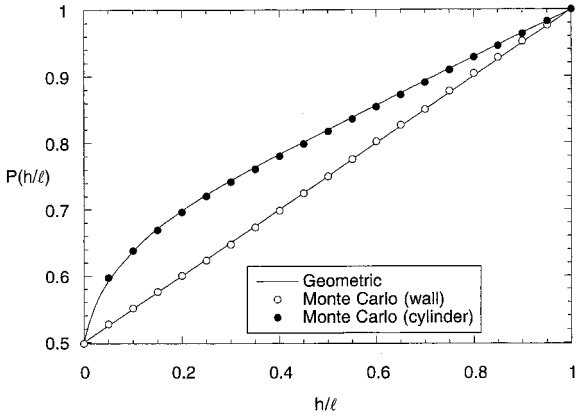

Figure 2. Probability of successfully placing one end of a dumbbell ($n = 2$) of length l at a distance h from a plane wall or a cylinder of radius $r_f = l$. The results obtained from purely geometric considerations are seen to agree with those computed using the Monte Carlo algorithm.

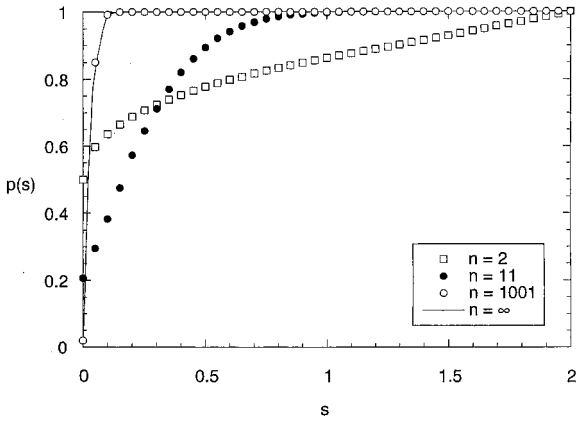

Figure 3. Probability that a freely jointed chain will not overlap with a fiber, if one end of the chain is placed at a dimensionless distance s ($=h/r_f$) from the fiber surface. Results are shown for chains with varying numbers of mass points (n), but with the same dimensionless contour length, $(n - 1)$-$l/r_f = 2$. The calculations with the continuum model ($n = \infty$) assumed that the dimensionless chain radius λ ($=r_g/r_f$) was 0.026, which is the same λ as for the chain with $n = 1001$.

The Monte Carlo and geometrical results for the wall and cylinder cases are compared in Figure 2. As one would expect, the wall and cylinder yielded the same limiting values of p. That is, exactly half of the rod orientations were allowed ($p = {}^1/_2$) for $h/l \rightarrow 0$, whereas all were allowed ($p = 1$) for $h/l \geq 1$. Excellent agreement between the Monte Carlo and geometrical results was found in both cases, which confirms that the chain-generation and test-fitting algorithms both performed properly.

Results

The probability $p(s)$ of successfully placing the end of a freely jointed chain at a dimensionless distance s from a fiber is shown in Figure 3. Results are given for molecules with varying numbers of mass points (n), but identical dimensionless contour lengths, $(n - 1)l/r_f$. In each case $p \rightarrow 1$ when s is large enough to make steric interactions negligible. The progressive reductions in p seen for smaller s reflect the fact that steric exclusion is more likely for a molecule placed closer to a fiber. Note that the spatial variations in p for "coarse" chains (small n) were found to be much more gradual than those for "fine" chains (large n). That is, increases in n both reduced $p(0)$ and caused p to approach unity more rapidly as s was increased. Consistent with the "absorbing wall" boundary condition used in the continuum calculations (eq 13), the Monte Carlo results for $n = 1001$ gave $p(0) \cong 0$. As shown, the entire curve for this case was in close agreement with the continuum result computed using the same radius of gyration.

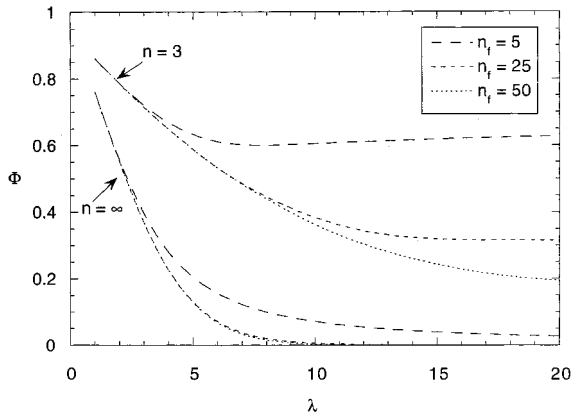

Figure 4. Effect on partitioning of the number of fibers assumed to be interacting with a single chain (n_f). The partition coefficients for a two-segment chain ($n = 3$) and for the continuum limit ($n = \infty$) are plotted as a function of the radius of gyration divided by the fiber radius ($\lambda = r_g/r_f$). Results are shown for three values of n_f, at a fixed volume fraction of fibers ($\phi = 0.06$). For $n = \infty$, the curves for $n_f = 25$ and 50 are indistinguishable.

An important issue in computing the partition coefficient (Φ) is the number of terms required in the product in eq 4, which corresponds to the number of neighboring fibers which have some influence on steric exclusion. Values of Φ for freely jointed chains are shown in Figure 4 as a function of λ ($=r_g/r_f$), based on 5, 25, or 50 fibers. Results are given for a two-segment chain ($n = 3$) and for the continuum case ($n = \infty$), at a fixed fiber volume fraction. As expected, Φ tended to decrease with increasing λ for either value of n. For a given λ, the partition coefficient was much smaller for the continuum model. The curves shown for varying numbers of fibers indicate that the number of terms needed to obtain a convergent value of Φ increases with increasing λ. For the two-segment chain, 25 fibers were adequate only for $\lambda < 8$, whereas for the continuum case, 25 were sufficient for λ of at least 20. (On this plot, the results for 25 or 50 fibers with $n = \infty$ are indistinguishable.) More fibers are needed for smaller n because of the more gradual spatial variations in p (Figure 3). The increase in Φ at large λ that is seen in Figure 4 for $n = 3$ and either 5 or 25 fibers is apparently an artifact caused by an inadequate number of terms in eq 4. Except where noted otherwise, in all subsequent results the number of terms was large enough to make the estimated truncation error <2% of Φ.

The dependence of the partition coefficient on fiber volume fraction and molecular size is shown in Figure 5. The partition coefficient is plotted here as a function of ϕ for several values of λ, using results obtained with the continuum model. As expected, for any given λ there was a monotonic decrease in Φ with increasing ϕ; that is, increasing the concentration of fibers enhances the steric exclusion of random-flight polymers, as it does for spheres (eq 1). For any given ϕ, Φ decreased with increasing λ, as seen already in Figure 4.

Figure 6 shows the effects of λ and n on Φ, with the fiber volume fraction held constant. (This plot is similar

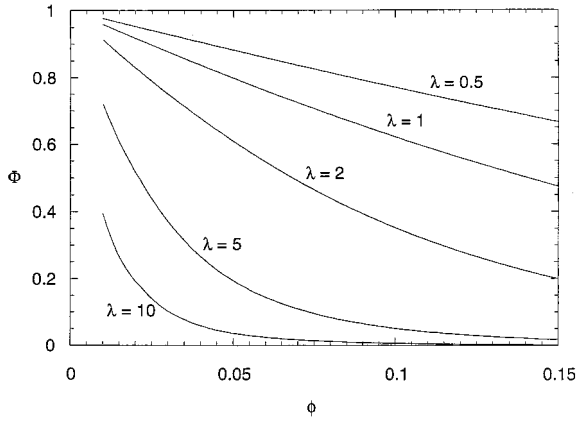

Figure 5. Effects of fiber volume fraction (ϕ) and relative molecular size (λ) on the partitioning of freely jointed chains, based on the continuum model ($n = \infty$).

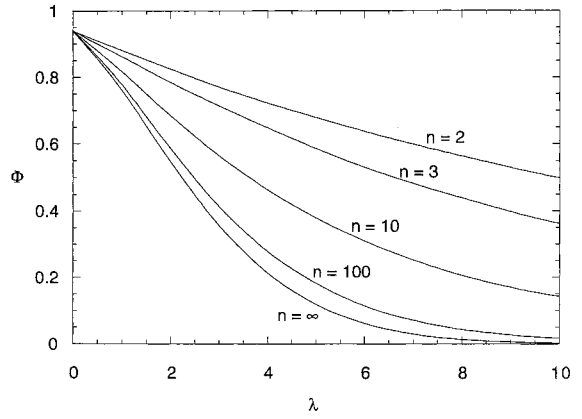

Figure 6. Effects of relative molecular size and number of mass points on the partitioning of freely jointed chains. For all curves $\phi = 0.06$.

to Figure 4, except that results are shown for more values of n, and 90 fibers were used in each case.) As mentioned before, Φ decreases with increasing n at any given λ. This is qualitatively similar to the results for random-flight polymers in cylindrical pores;[8] the parameter in a pore model that is analogous to λ is the radius of gyration divided by the pore radius. The Monte Carlo results for $n = 1000$ (not shown) closely approached those for the continuum model, verifying that the two approaches are complementary.

Figure 7 shows the effects of the bond angle (β) and n on Φ (with λ and ϕ held constant). For any constant value of n, the partition coefficient first decreased, and then increased, as the bond angle was increased from 0 to 180°. Similar to the trend seen in Figure 6 for random-flight chains, Φ decreased with increasing n for any fixed, nonzero bond angle. The special case of $\beta = 0$, where the chain folds back on itself at each step, corresponds to a dumbbell. Thus, the partition coefficient for $\beta = 0$ and any even value of n is identical to that for a random-flight chain with $n = 2$. At $\beta = 180°$ and with $n \rightarrow \infty$, the molecule becomes a solid rod. Because the mass of a rod is distributed uniformly thoughout its length, whereas the mass of the dumbbell is concentrated at the ends, r_g for a rod is smaller (by a factor $1/\sqrt{3}$) than that for a dumbbell of equivalent length. Thus, for equal values of λ, the rod must be longer, which makes Φ smaller (0.51 vs 0.69 for the conditions of Figure 7). The minimum values of Φ for a given n correspond to bond angles where the contour

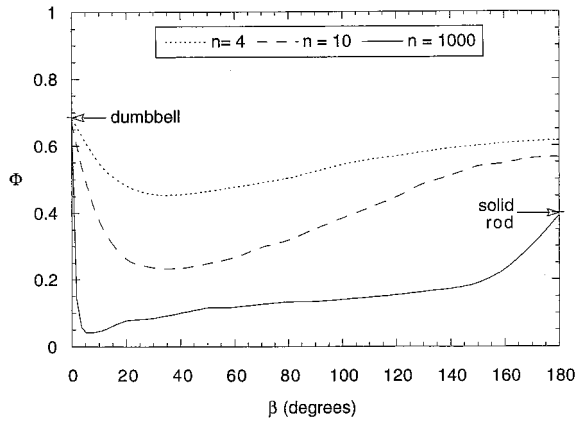

Figure 7. Effects of bond angle (β) and number of mass points on the partition coefficient. In all cases $\lambda = 5$ and $\phi = 0.06$. The arrows indicate the limiting results for a dumbbell ($n = 2$, $\beta = 0$) and a solid rod ($n = \infty$, $\beta = 180°$).

length of the chain is maximized. The results in Figure 7 suggest that, for $n \rightarrow \infty$, the partition coefficient would increase monotonically with increasing β (excluding the singularity at $\beta = 0$).

The Monte Carlo results for random-flight chains are represented accurately by

$$\Phi = \exp[-(1 + \pi^a \lambda^b)\phi] \tag{17}$$

$$a = 1 - \exp\left[-\frac{n-2}{4}\right] \tag{18}$$

$$b = \frac{3}{2} - \frac{1}{2}\exp\left[-\frac{\sqrt{n-2}}{8}\right] \tag{19}$$

These empirical expressions gave values of Φ which were within 0.03 or within 10% of the Monte Carlo result for Φ (whichever was smaller) for all combinations of parameters in Figures 5 and 6. The Monte Carlo results for a fixed bond angle can be obtained by representing that chain as an equivalent random-flight chain. This is done by matching the radius of gyration and contour length of the two chains, as in the Kuhn representation (see Discussion).

Discussion

In this study we have extended the fiber−matrix partitioning model of Ogston[1] to encompass flexible polymeric solutes. The fibrous material is envisioned as an array of rigid cylinders with random orientations, as in the analysis of Ogston, but the solutes are random-flight chains or linear chains with bond angle restrictions, rather than rigid spheres. To our knowledge, this work provides the first theoretical predictions for the partitioning of flexible, linear polymers in fibrous membranes or gels. Several published sets of data on the partitioning of linear polymers in hydrogels provide an opportunity to test the theoretical predictions. Accordingly, this section is devoted mainly to comparisons of our theory with the available data.

Dubin et al.[17] and Hussain et al.[18] measured Φ for pullulan, a linear polysaccharide, in Superose 6 and Superose 12 (agarose) chromatography media, respectively. Data in polyacrylamide gels include those of Tong and Anderson[19] for poly(ethylene glycol) (PEG), and those of Williams et al.[20] for dextran, a polysaccharide with varying amounts of branching.

Table 1. Properties of Hydrogels Used in Partitioning Experiments[a]

authors	gel	r_f (nm)	ϕ
Dubin et al.[17]	superose 6 (agarose)	1.9	0.06
Hussain et al.[18]	superose 12 (agarose)	1.9	0.12
Tong and Anderson[19]	polyacrylamide	0.33−0.43	0.02−0.14
Williams et al.[20]	polyacrylamide	0.33−0.43	0.03−0.08

[a] See text for sources for parameter values.

Table 1 summarizes the properties of the gels used in the experimental studies to be discussed. The important gel parameters in steric partitioning are the fiber radius, r_f, and fiber volume fraction, ϕ. The value of $r_f = 1.9$ nm for agarose is a number-average of fiber radii reported by Djabourov et al.,[21] based on SAXS data. They found that roughly 87% of the fibers in an agarose gel have a radius of 1.5 nm, while the remaining 13% have a radius of 4.5 nm. On the basis of the atomic structure of polyacrylamide, Weiss and Silberberg[22] estimated a fiber radius of 0.33 nm for that polymer. To allow for the possibility that the effective fiber radius may be increased by the association of water molecules with polyacrylamide, we computed results using $r_f = 0.43$ nm as well as 0.33 nm. (Because r_f for agarose is much larger, a similar 0.1 nm increase would have negligible effect on the predicted partition coefficients.) Volumes fractions in the agarose gels ranged from 0.06 to 0.12, while those in the polyacrylamide gels were 0.02−0.14.

In keeping with the theory, the polymeric solutes were represented either as freely jointed chains or as chains with fixed bond angles. In addition to the bond angle (if used), each chain was characterized by two independent parameters. One of these was always the measured radius of gyration (r_g). Among the possible choices for the remaining independent parameter are (i) the segment length (l), (ii) the number of mass points (n), and (iii) the contour length [$(n - 1)l$]. For freely jointed chains, we used either l or $(n - 1)l$. When l was the parameter of choice, it was equated with the persistence length of the polymer and denoted as l_p; the corresponding number of mass points (computed from r_g and l_p) is denoted as n_p. When the contour length was specified, as suggested by Kuhn (see Kratky[23]), we set $(n - 1)l = (l_m M)/M_m$ where M is the polymer molecular weight, M_m is the monomer molecular weight, and l_m is the length of a monomer. For chains with fixed bond angles we tried all three approaches: equating segment length with monomer length ($l_\beta = l_m$), computing n from the degree of polymerization ($n_\beta = M_w/M_m + 1$), or fixing the contour length as described above. It was found that the Kuhn and fixed-bond-angle representations gave virtually identical partition coefficient predictions, so that the Kuhn results are not shown in the figures that follow. Also, the fixed-bond-angle model gave the same results using all three approaches for selecting the final parameter. In presenting the results for that model, n will be treated as the specified parameter.

Table 2 lists the parameter values for the solutes under consideration. For PEG with molecular weights of 5 and 12.6 kDa, $r_g = 2.2$ and 3.6 nm, respectively.[24] The persistence length of PEG was taken to be 0.9 nm,[24] the bond angle used was 110°,[10] and the monomer molecular weight is 44 Da. For pullulan, r_g was obtained by extrapolating a least-squares fit to the r_g vs M data of Kato et al.[25] and Nordmeier.[26] Most of the estimates of pullulan persistence length cluster around 1.6 nm.[27,28] The bond angle (β) was taken to be 116°, [29] and the monomer molecular weight is 312 Da. The dextrans studied by Williams et al.[20] had Stokes−Einstein radii ranging from 1.5 to 8.7 nm. The corresponding range of r_g was estimated as 2.2−11.3 nm.[30] The persistence length for dextran is 2−3 nm, the larger values of l_p corresponding to the smaller molecular weights.[31] The bond angle used for dextran was 116°,[29] and the monomer molecular weight is 228 Da. In each case the estimates of n were rounded to the nearest integer.

The predicted partition coefficients are compared with the data of Tong and Anderson[19] for PEG/polyacrylamide in Figures 8 and 9. Each plot shows the effects of variations in fiber volume fraction, for a single solute size. It is seen that the calculated partition coefficients were affected less by the choice of model used to represent PEG (freely jointed chain or chain with fixed bond angle) than by the assumed fiber radius. The best results were obtained with the larger fiber radius, which corresponds roughly to a polyacrylamide chain surrounded by a monolayer of associated water. The predictions were somewhat more accurate for the smaller PEG (Figure 8).

Figure 10 compares the predictions for pullulan/agarose with the data of Dubin et al.[17] and Hussain et al.[18] For each of these sets of data, the independent variable was solute size. Because the freely jointed chain and the chain with fixed bond angles gave virtually the same results, only the latter curves are shown. It is seen that the predictions were accurate for the smaller pullulans ($\lambda < 3$) but that the theory tended to underestimate Φ for the larger sizes. One possible source of error in the predictions is that we modeled agarose as an array of fibers with a uniform radius, whereas (as discussed above) SAXS data suggest that the actual distribution of fiber radii is bimodal. However, for spherical molecules of comparable size to the pullulans considered here, Φ has been calculated to decrease by about 10% if a two-fiber representation of agarose is used. Thus, the effects of a mixture of fiber sizes are expected to be small in this case and in the wrong direction to explain the discrepancies in Figure 10.

The predicted values of Φ for dextran/polyacrylamide are compared with the data of Williams et al.[20] in Figures 11 and 12. Each plot is based on variations in molecular size, with a fixed volume fraction of fibers. (The comparisons shown are for $\phi = 0.03$ or 0.06 only; the results for $\phi = 0.08$ are qualitatively similar.) For the dextrans the parameter values were such that there was a very noticeable difference between the results for freely jointed chains and chains with a fixed bond angle, with the former giving larger predicted values of Φ. Neither model performed well over a large range of molecular sizes, although the freely jointed chain (using the persistence length) gave reasonably good results for the smaller dextrans ($r_g < 3$ nm). As with the pullulan/agarose system, the predicted values of Φ underestimated what was measured for the larger dextrans. Data for even larger dextrans were reported by Williams et al., but the maximum number of fibers we could accommodate ($n_f = 90$, due to computer limitations) confined the range of sizes to what is shown in Figures 11 and 12.

It is not entirely surprising that the results were poorest for dextran, in that dextran is the least ideal of

Table 2. Properties of Test Solutes Used in Partitioning Experiments[a]

authors	solute	M (kDa)	r_g (nm)	n_p l_p (nm)	n_β l_β (nm)	β (deg)
Tong and Anderson[19]	PEG	5−12.6	2.2−3.6	30−90 0.9	120−290 0.3	110
Dubin et al.,[17] Hussain et al.[18]	pullulan	5−200	2.1−17	10−700 1.6	20−610 1.1	116
Williams et al.[20]	dextran	2−160	2.2−11.3	3−170 2−3	10−700 0.7−1.0	116

[a] See text for sources for parameter values.

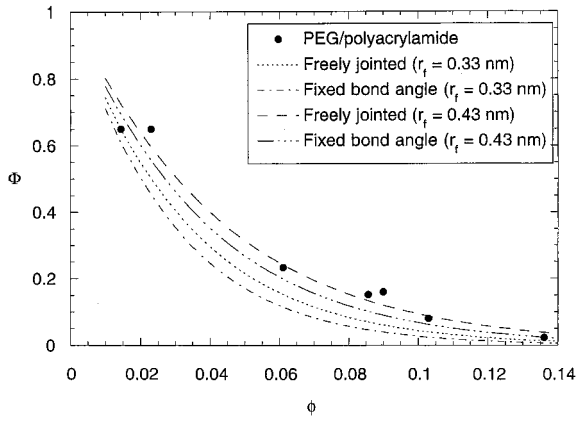

Figure 8. Measured and predicted partition coefficients of 5 kDa PEG in polyacrylamide gels of varying concentration. The symbols are the data of Tong and Anderson.[19] The curves are the Monte Carlo predictions for a freely jointed chain ($n = 33$) or a chain with a bond angle of 110° ($n = 115$). In each case the calculations were done for "bare" ($r_f = 0.33$ nm, $\lambda = 6.6$) and "hydrated" ($r_f = 0.43$ nm, $\lambda = 5.1$) polyacrylamide; see text for details of parameter estimation.

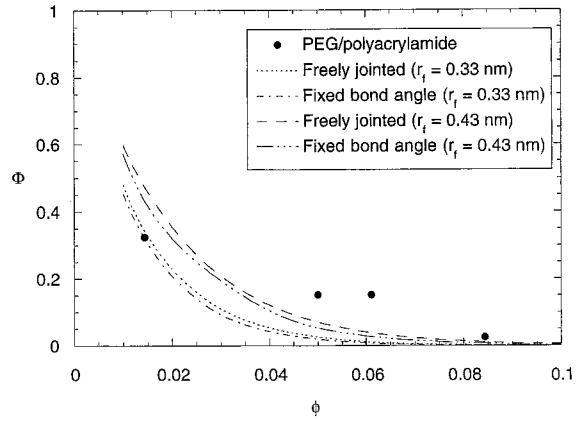

Figure 9. Measured and predicted partition coefficients of 12.6 kDa PEG in polyacrylamide gels of varying concentration. The symbols are the data of Tong and Anderson.[19] The curves are the Monte Carlo predictions for a freely jointed chain ($n = 89$) or a chain with a bond angle of 110° ($n = 287$). In each case the calculations were done for "bare" ($r_f = 0.33$ nm, $\lambda = 11$) and "hydrated" ($r_f = 0.43$ nm, $\lambda = 8.4$) polyacrylamide; see text for details of parameter estimation.

the test solutes considered. In particular, the branching of this polysaccharide becomes progressively more prominent as its molecular weight increases.[32] That the behavior of dextran is anomalous is suggested by the results in Figure 13, which compares partitioning data for PEG, pullulan, and dextran in gels with $\phi = 0.06$. The curves shown are predictions for a solid rod and for a freely jointed chain with many segments. Whereas the PEG/polyacrylamide and pullulan/agarose data are seen to follow much the same relationship between Φ and λ, the values of Φ for dextran are much larger,

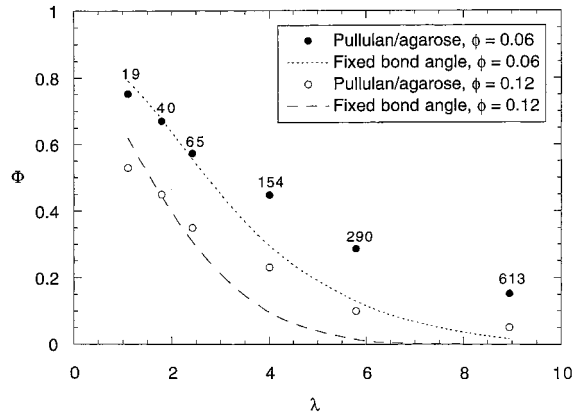

Figure 10. Measured and predicted partition coefficients of pullulans of varying size in agarose gels. The symbols are the data of Dubin et al.[17] and Hussain et al.[18] for $\phi = 0.06$ and $\phi = 0.12$, respectively. The curves are Monte Carlo predictions for a bond angle of 116° and $r_f = 1.9$ nm. The number of mass points increased with increasing molecular size, as indicated.

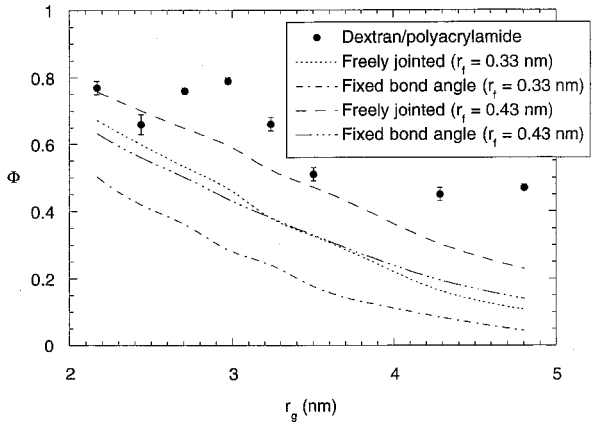

Figure 11. Measured and predicted partition coefficients of dextrans of varying size in polyacrylamide gels with $\phi = 0.03$. The symbols are the data of Williams et al.[20] The curves are the Monte Carlo predictions for a freely jointed chain ($n = 3-20$) or a chain with a bond angle of 116° ($n = 14-92$).

falling near (or above) the limiting curve for a solid rod.

It should be noted that the present theory does not account for the effects of solvent quality. For example, a polymer with given values of bond angle and monomer length will have a radius of gyration given by eq 3 only under Θ conditions. However, it was found that, for PEG, specifying the measured value of r_g and setting $l = l_m$ gave a value of $n - 1$ that was quite close to the actual degree of polymerization. Reasonable consistency was obtained also with pullulan. This indicates that applying eq 3 to PEG or pullulan (each in water) led to minimal errors. The calculated value of $n - 1$ for dextran was much less satisfactory, probably due to its branched structure.

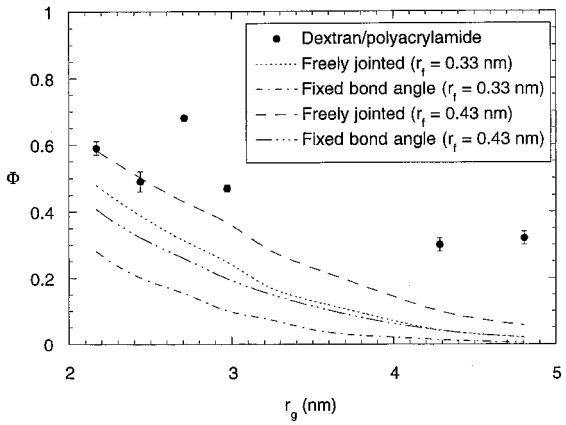

Figure 12. Measured and predicted partition coefficients of dextrans of varying size in polyacrylamide gels with $\phi = 0.06$. The symbols are the data of Williams et al.[20] The curves are the Monte Carlo predictions for a freely jointed chain (n = 3−20) or a chain with a bond angle of 116° (n = 14−92).

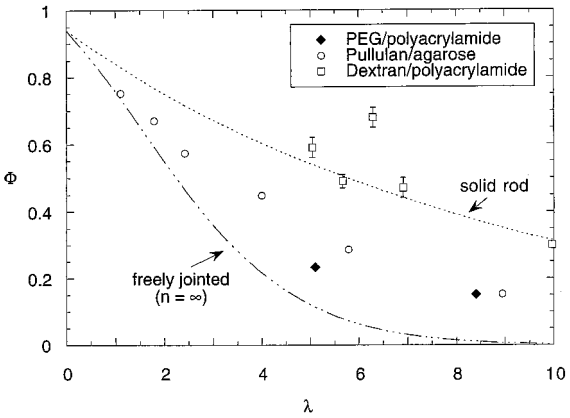

Figure 13. Comparison of the partitioning of various polymers in gels with $\phi = 0.06$. The symbols are the data of Tong and Anderson,[19] Dubin et al.,[17] and Williams et al.[20] for PEG/polyacrylamide, pullulan/agarose, and dextran/polyacrylamide, respectively. The curves shown are limiting results for a solid rod ($n = \infty, \beta = 180°$) and for a freely jointed chain with many segments ($n = \infty$, β unrestricted).

In summary, we have developed a theory for the equilibrium partitioning of dilute solutions of flexible, linear polymers in fibrous membranes and gels. In this theory the fibrous material or gel is characterized by two parameters, the fiber radius and fiber volume fraction, and the polymeric solutes are described by a radius of gyration, a number of mass points per chain, and (if desired) a bond angle. Although the fibrous material and flexible polymer were each represented very simply, and only steric interactions were considered, the theory was found to be moderately successful in predicting experimental values of partition coefficients.

Acknowledgment. This work was supported by Grant DK20368 from the National Institutes of Health. J.A.W. is the recipient of a National Science Foundation Graduate Fellowship.

References and Notes

(1) Ogston, A. G. *Trans. Faraday Soc.* **1958**, *54*, 1754.
(2) Fanti, L. A.; Glandt, E. D. *J. Colloid Interface Sci.* **1990**, *135*, 385, 396.
(3) Lazzara, M. J.; Blankschtein, D.; Deen, W. M. *J. Colloid Interface Sci.* **2000**, *226*, 112.
(4) Johnson, E. M.; Deen, W. M. *J. Colloid Interface Sci.* **1996** *178*, 749.
(5) Cassasa, E. F. *J. Polym. Sci., Polym. Lett. Ed.* **1967**, *5*, 773.
(6) Lin, N. P.; Deen, W. M. *Macromolecules* **1990**, *23*, 1990.
(7) Chandrasekhar, S. *Rev. Mod. Phys.* **1943**, *15*, 1.
(8) Davidson, M. G.; Suter, U. W.; Deen, W. M. *Macromolecules* **1987**, *20*, 1141.
(9) Kramers, H. A. *J. Chem. Phys.* **1946**, *14*, 415.
(10) Flory, P. J. *Principles of Polymer Chemistry*; Cornell University Press: Ithaca, NY, 1953; pp 415, 430.
(11) Meyer, P. L. *Introduction to Probability and Statistical Applications*; Addison-Wesley Publishing: Reading, MA, 1965; p 149.
(12) Press, W. H.; Flannery, B. P.; Teukolsky, S. A.; Vetterling, W. T. *Numerical Recipes in Fortran*, 2nd ed.; Cambridge University Press: Cambridge, MA, 1986; pp 272−273, 838−842.
(13) DiMarzio, E. A. *J. Chem. Phys.* **1965**, *42*, 2101.
(14) Jaeger, J. C. *J. Math. Phys.* **1956**, *34*, 316.
(15) Allen, M. P.; Tildesley, D. J. *Computer Simulation of Liquids*; Clarendon Press: Oxford, 1987; p 349.
(16) Harris, D. C. *Quantitative Chemical Analysis*, 3rd ed.; W. H. Freeman and Company: New York, 1991; p 43.
(17) Dubin, P. L.; Edwards, S. L.; Mehta, M. S.; Tomalia, D. *J. Chromatogr.* **1993**, *635*, 51.
(18) Hussain, S.; Mehta, M. S.; Kaplan, J. I.; Dubin, P. L. *Anal. Chem.* **1991**, *63*, 1132.
(19) Tong, J.; Anderson, J. L. *Biophys. J.* **1996**, *70*, 1505.
(20) Williams, J. C.; Mark, M. A.; Eichholtz, S. *Biophys. J.* **1998**, *75*, 493.
(21) Djabourov, M.; Clark, A. H.; Rowlands, D. W.; Ross-Murphy, S. B. *Macromolecules* **1989**, *22*, 180.
(22) Weiss, N.; Silberberg, A. *Br. Polym. J.* **1977**, *9*, 144.
(23) Kratky, O. *Pure Appl. Chem.* **1966** *12*, 483.
(24) Kawaguchi, S.; Imai, G.; Suzuki, J.; Miyahara, A.; Kitano, T.; Ito, K. *Polymer* **1997**, *38*, 2885.
(25) Kato, T.; Katsuki, T.; Takahashi, A. *Macromolecules* **1984**, *17*, 1726.
(26) Nordmeier, E.; Xing, H.; Lechner, M.-D. *Makromol. Chem.* **1993**, *194*, 2923.
(27) Adolphi, U.; Kulicke, W.-M. *Polymer* **1997**, *7*, 1513.
(28) Muroga, Y.; Yamada, Y.; Noda, I.; Nagasawa, M. *Macromolecules* **1987**, *20*, 3003.
(29) Arnott, S.; Scott, W. E. *J. Chem. Soc., Perkin Trans.* **1972**, *2*, 324.
(30) Nordmeier, E. *J. Phys. Chem.* **1993**, *97*, 5770.
(31) Garg, S. K.; Stivala, S. S. *J. Polym. Sci., Polym. Phys. Ed.* **1978**, *16*, 1419.
(32) Bovey, F. A. *J. Polym. Sci.* **1959**, *35*, 167.

MA0008793